

NON-HEME IRON C-H OXIDATION: TOLERANCE OF NITROGEN-CONTAINING MOTIFS WITH APPLICATION
TO AMINO-ACID AND PEPTIDE OXIDATION

BY

GREGORY S SNAPPER

THESIS

Submitted in partial fulfillment of the requirements
for the degree of Master of Science in Chemistry
in the Graduate College of the
University of Illinois at Urbana-Champaign, 2013

Urbana, Illinois

Adviser:

Professor M. Christina White

ABSTRACT

Direct oxidation of C-H bonds using non-heme iron catalysis has proven to be a highly useful transformation since its development in recent years. The ability to directly install oxygen into a hydrocarbon framework negates the need for pre-oxidized materials, and allows for quick and efficient access to more diverse and complex molecules; in some cases, access to motifs that would not otherwise be accessible is possible. Furthermore, ligation at the iron center with a tetra-dentate amine complex containing two adjacent, equatorial active sites on the metal has allowed for synthetically useful levels of reactivity, with the added benefit of predictable selectivity and even directing group effects. In addition, the PDP ligand framework has been shown amenable to various steric and electronic modifications, allowing for tuning of reactivity and selectivity. Key limitations are still prevalent in the methodology, however, including lack of an enantioselective variant, and little/no tolerance of certain common functional groups including amines and most aromatic rings. This work describes development of novel substrate protection methods to address the functional group tolerance of nitrogen-containing substrates, with further application to oxidation of amino-acids and small peptides.

Due to inherent catalyst reactivity and reaction conditions, highly complex molecules with a variety of functional groups remain challenging for C-H oxidation, a process that is highly desired in academic and industrial settings alike. The inherent ligation capabilities of nitrogen to iron (exemplified by the tetra-amine PDP ligand) obviate the difficulty in tolerating a substrate containing any variety of amine motifs. Novel protection strategies using various electron-withdrawing group on nitrogen were developed which prevent this ligation, and allow for productive oxidation at distal sites on the molecule. Due to the abundance of various classes of amines, different protective group strategies were developed, depending on which type of amine was present.

Application of these protective schemes was then applied to amino-acid and peptide settings. An added benefit of an ester moiety adjacent to the amine allowed for simple nitrosulfonyl protection, whereby oxidation of aliphatic side chain residues was possible. In other cases, certain residues were found to be oxidatively stable. In dipeptide settings, selectivity trends were studied between various residues, and it was also found that residue position (N- vs. C- terminus) greatly affected reactivity trends. Overall this process has been shown to greatly surpass current state of the art methods for amino-acid and peptide oxidation/diversification, and increases the synthetic potential for development of pharmaceuticals of this variety.

TABLE OF CONTENTS

CHAPTER 1: IMPROVING FUNCTIONAL GROUP TOLERANCE OF NON-HEME IRON C-H OXIDATION VIA NOVEL SUBSTRATE PROTECTIVE GROUP STRATEGIES.....	1
1.1 Introduction.....	1
1.2 Results and Discussion.....	3
1.3 Conclusions.....	8
1.4 Experimental Section.....	8
1.5 References.....	13
CHAPTER 2: APPLICATION TOWARDS AMINO ACID AND PEPTIDE OXIDATION, WITH FOCUS ON REACTIVITY AND SELECTIVITY TRENDS.....	14
2.1 Introduction.....	14
2.2 Results and Discussion.....	15
2.3 Conclusions.....	23
2.4 Experimental Section.....	24
2.5 References.....	32

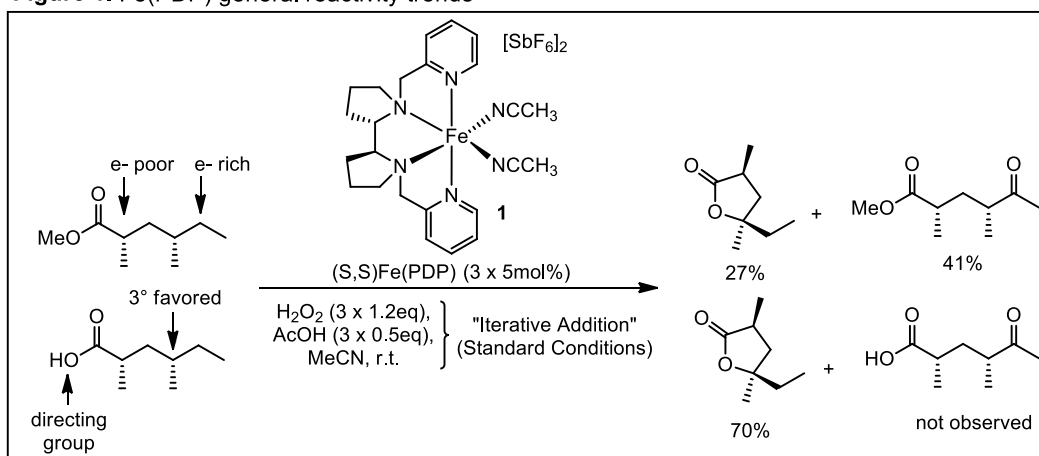
CHAPTER 1

IMPROVING FUNCTIONAL GROUP TOLERANCE OF NON-HEME IRON C-H OXIDATION VIA NOVEL SUBSTRATE PROTECTIVE GROUP STRATEGIES

1.1 INTRODUCTION

The C-H bond is increasingly being viewed as a new functional group, with the potential to be transformed selectively to C-O, C-N, and even C-C bonds.¹ Of particular interest in our group is the formation of C-O bonds, which are prevalent in many natural products and pharmaceutical compounds.² The non-heme, small molecule Fe-catalyst developed in our group is a novel tool for oxidation of unactivated C-H bonds, owing to its mild conditions and predictable selectivities.³ As previously reported, Fe(PDP) **1** selects for: 1) 3° C-H bonds in preference to 2° and 1° C-H bonds; 2) C-H bonds distal to electron-withdrawing functionality (electron-rich C-H bonds); and 3) sterically accessible C-H bonds. In addition, carboxylic acids were established to act as directing groups capable of overriding electronic preferences of the catalyst (Figure 1).

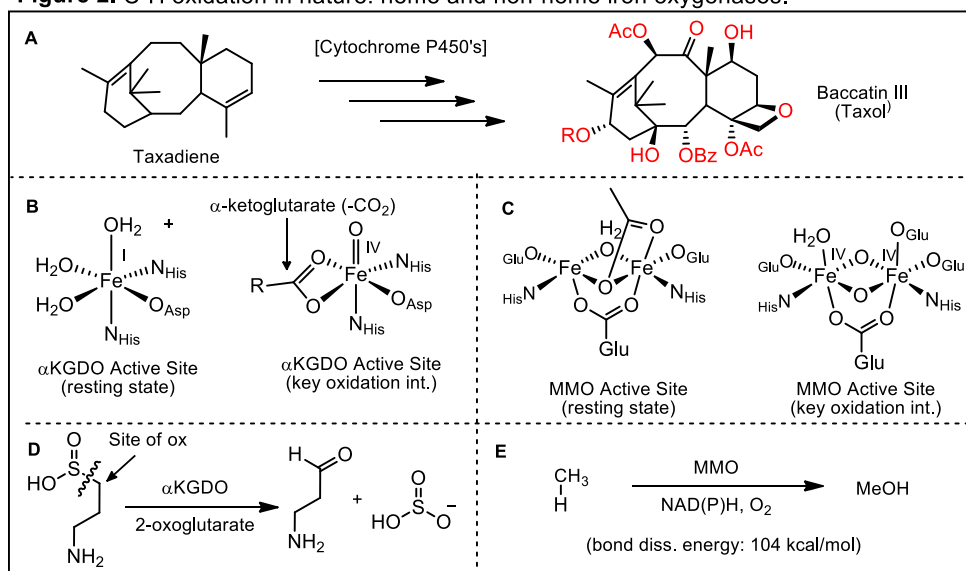
Figure 1. Fe(PDP) general reactivity trends



Late-stage C-H oxidation allows for efficient syntheses of complex small molecules by limiting the need for functional group manipulations (oxidations/reductions; protecting group introduction/removal). This direct installation of oxygen can be a powerful tool for construction of complex, highly functionalized motifs, both for synthetic streamlining as well as product diversification. A classic example of the ability of nature to build up densely functionalized motifs from relatively simple hydrocarbons is the biosynthesis of Taxol⁴ (Figure 2, A). After production of Taxadiene via a cyclase enzyme, >20 different heme-based Cytochrome P450 tailoring enzymes introduce oxygen functionality

around the periphery of the hydrocarbon core with incredible levels of site-, chemo-, and stereoselectivity *en route* to fully oxygenated Taxol^x. Other natural enzymes like Methane Mono Oxygenase (MMO) and α -Ketoglutarate Dependent Oxygenase (α KGDO) achieve similar reactivity utilizing non-heme supported iron centers within the enzyme (Figure 2, B and C). In these cases, a common motif is the “2-His-1-carboxylate triad”, where 2 Histidine residues and one carboxylate residue (Aspartic or Glutamic acid) support the iron center within the active site and throughout the oxidation process. Although α KGDO and MMO differ in the number of iron atoms present in the active site (mononuclear and dinuclear, respectively), each can support a high-spin iron(IV) oxo species capable of selective and difficult oxidations (Figure 2, D and E). In fact, MMO is one of the most intriguing of the natural non-heme oxo-enzymes due to its fascinating ability to transform a highly inert methane C-H bond (bond dissociation energy = 104 kcal/mol) into methanol, while over oxidation to formaldehyde is completely suppressed.

Figure 2. C-H oxidation in nature: heme and non-heme iron oxygenases.



Achieving biomimetic levels of reactivity and selectivity using non-enzymatic, small-molecule systems is an active area of research in many laboratories. While progress has been made with our non-heme iron catalyst, much remains to be explored in the area of substrate scope, with emphasis on functional group tolerance (FGT). To address this issue, we have explored rational catalyst design and novel protection strategies (substrate modification) to expand on current catalyst reactivity and selectivity capabilities. With these advancements, great progress has been made in the areas of alkaloid oxidation (nitrogen tolerance) with application to amino acid and peptide oxidation.

butyloxycarbonyl (Boc) protective group is appended, 0% of the corresponding hydroxylated product is isolated (Table 1, entry 1). Furthermore, no isolable amount of the starting material can be recovered, presumably due to substrate degradation via a boc-deprotection type pathway. Alternatively, use of a highly electron-withdrawing *p*-nitrophenylsulfonyl group (Nosyl) again affords none of the desired hydroxylated product (entry 2). In this case, a quantitative amount of the starting material can be recovered, suggesting catalyst ligation as opposed to N-deprotection. Combining the two in a dual protection strategy (N-Boc-N-Nosyl) resulted in restored reactivity, yielding the corresponding amino-alcohol **4** in 55% yield with 30% recovered starting material (entry 3). Additionally, we found that a “single” protective group, 4-nitrophthalimide, was sufficient for productive oxidation, affording amino-alcohol **5** in 57% yield and 27% recovered starting material.

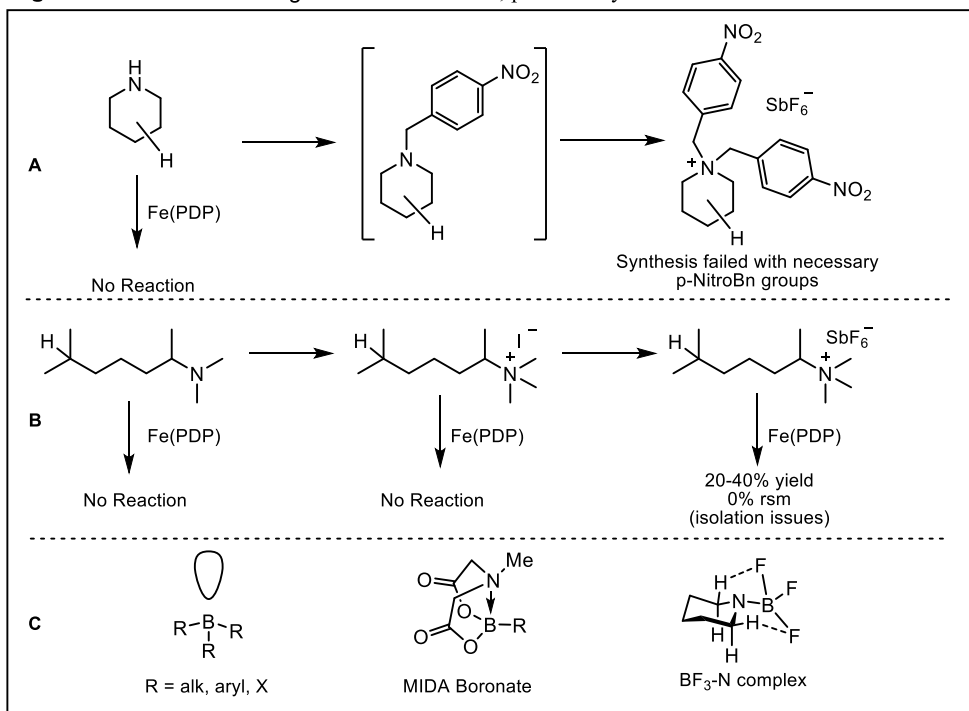
Table 1. Optimization of protective groups for primary amine substrate oxidation.

Entry	Product	rsm	yield	Entry	Product	rsm	yield
1		0%	0%	3		30%	55%
2		100%	0%	4		27%	57%

Protection of 2° and 3° linear and cyclic amines presents a new challenge in that the dual-protection strategy optimized for 1° amines is not possible. For 2° amines, we hypothesize a single protective group would need to impart large steric or electronic interference between the amine and the catalyst, while 3° amines would require a similar modification for a reasonable probability of oxidation to occur. In the case of piperidine, a cyclic 2° amine, a single Boc or Nosyl group would not be sufficient to afford reactivity (from trends in Table 1). Instead we envisioned a di-alkylation strategy using a *p*-nitrobenzyl group that would lead to the corresponding ammonium complex (Figure 4, A). Although literature precedence existed for alkylation using a simple benzyl halide⁵, the required *p*-nitrobenzyl variant was unable to undergo the second alkylation and was therefore not able to be tested. A similar ‘alkylation-to-ammonium’ strategy was implemented for a 3° amine, this time using methyl iodide, followed by counterion metathesis (Figure 4, B). While neither the original amine nor the

ammonium iodide productively converted to hydroxylated product, metathesis to the SbF_6^- salt followed by oxidation did afford the corresponding amino-alcohol (20-40% yields). Due to the extremely polar nature of the ammonium salt, isolation on silica was inconsistent and challenging, and yields varied dramatically. Another potential problem with this method is the deprotection. Although removal of a single methyl group from the ammonium salt is precedented^x, reaction conditions are harsh and yields are typically low.

Figure 4. Protective strategies for 2°/3° amines; preliminary oxidation observations.



While standard covalent modification appeared to be ineffective for these challenging amine classes, we hypothesized that complexation of the lone-pair via Lewis-type interactions could be a viable alternative. We became interested in boron due to its Lewis-acid nature and high aza-philicity⁷. The empty p-orbital on tri-substituted boron compounds is known to interact with Lewis-basic lone pairs, especially those of amines. Furthermore, the three R groups can be a variety of substituents of varying steric and electronic properties (Figure 4, C). MIDA boronates exemplify this type of attenuation of reactivity through similar interactions. Developed by the Burke group for iterative cross-coupling reactions⁸, the nitrogen lone-pair of the MIDA group donates into the empty p-orbital on boron, preventing transmetalation until the MIDA group is hydrolyzed and the empty p-orbital re-exposed⁸. In the case of a C-H oxidation system, complexation of a highly electron-deficient boron source (BF_3) to an amine would hopefully effect a similar outcome, whereby the nitrogen would remain complexed to the

boron source rather than the metal center of the catalyst. Additionally, use of a highly electron-withdrawing source of boron would also limit the probability of α -oxidation to the hemiaminal.

Historically, BF_3 has been used as an *in-situ* Lewis-acid activator for various reactions⁷. However, it is atypical that the complex itself is isolated, purified, and used as a reagent. For our purposes, isolation of the pure complex was necessary in order for testing under the oxidation conditions such that no free amine remained to inhibit catalyst activity. Table 2 outlines efforts towards nitrogen protection with BF_3 . 1° amines are successfully complexed and purified, producing complexes **6a** and **7a** in useful yields of the pure, isolated complex (entries 1 and 2). Similarly, 2° cyclic amines also afford the corresponding complexes **8a** and **9a** in excellent yields, and are stable to silica gel chromatography (entries 3 and 4). In the case of diamine **9**, use of limiting BF_3 (1 equiv) resulted in complete selectivity for complexation at the 2° nitrogen, with no bis- BF_3 complex observed by TLC or upon isolation (entry 4).

Table 2. Synthesis and isolation of (N)- BF_3 amine complexes.

$\text{R}-\text{N}(\text{R}')-\text{R}'' \xrightarrow[\text{Et}_2\text{O, -78C to r.t.}]{\text{BF}_3 \cdot \text{OEt}_2} \text{R}-\text{N}(\text{R}')(\text{R}'')-\text{BF}_3$									
Entry	Substrate	product	Yield	Isolable ^a	Entry	Substrate	product	Yield	Isolable ^a
1			55%	yes	5			0%	no
2			93%	yes	6			0%	no
3			94%	yes	7			47%	no ^b
4			91%	yes	8			87%	yes ^c

a) "Isolable" signifies that the complex does not decompose on silica during chromatography, and is relatively stable to benchtop storage. b) isolable by filtration of the crude complexation mixture, but not stable to silica gel chromatography. c) Stable on Florisil but not Silica.

When two equivalents of BF_3 are used, however, no amount of bis-complexed **10a** can be isolated (entry 5). Similarly, complexation of 3° amine **11** resulted in conversion by TLC to the presumed N- BF_3 complex **11a**. However upon attempts to isolate and purify the complex, degradation to the free amine was immediate and unavoidable (entry 6). In the case of a 3° aryl amine (pyridine, **12**), a 47%

yield of the pure complex was achieved via crystallization and filtration. (When subjected to silica gel chromatography, the complex readily dissociated). Complexation with quinuclidine **13** afforded 87% of complex **13a**, also isolated via crystallization/filtration. As with **12a**, this complex was unstable to normal silica gel, but was found to be stable to the less-acidic Florisil. From these results, it is apparent that 1° and 2° amines are synthetically ideal substrates for BF₃ complexation/protection, while isolation and purification issues prevent this methodology from applying generally to 3° amines.

With several BF₃-complexed amines available, we began testing their stability to oxidation (Table 3). Oxidation of 4-isoamyl piperidine-BF₃ yielded amino-alcohol **14** (as the BF₃ complex) in 45% yield, with 40% recovered starting material (entry 1). The high recovered starting material and overall mass balance of this reaction suggest a high level of site selectivity, even in the presence of 6 labile C-H bonds. As predicted, no amount of hemiaminal was detected in the reaction due to the extremely electronegative nature of the complex, with oxidation deferred several bonds away from the N-BF₃ complex. Further evidence of this can be seen in entry 2, whereby oxidation of n-hexylamine-BF₃ yielded a modest 25% of ketone **15** (5 carbons removed from the nitrogen) with 44% of the starting material recovered (entry 2). The only isolable side-product of this reaction is oxidation at site 2, resulting in 8% of ketone **16**, with negligible amounts of combined oxidation at the 3 interior carbons. Since methylene oxidation is typically more difficult for this catalyst than methine C-H bonds, we also tested isoamylamine-BF₃ (entry 3). Although a low mass balance was achieved overall, the corresponding amino-alcohol was produced in 22% yield, with 19% recovered starting material (entry 3). Comparison of the yields of entries 1 and 3 further demonstrates the electronic influence of the BF₃ group, where oxidation 3 carbons removed is significantly inhibited compared to 7 carbons away. This is further exemplified by oxidation of quinuclidine-BF₃ **18** (2 carbons distant), where no oxidation products are observed, and >90% of the starting material can be recovered (entry 4).

Table 3. Oxidation of BF₃-protected amines

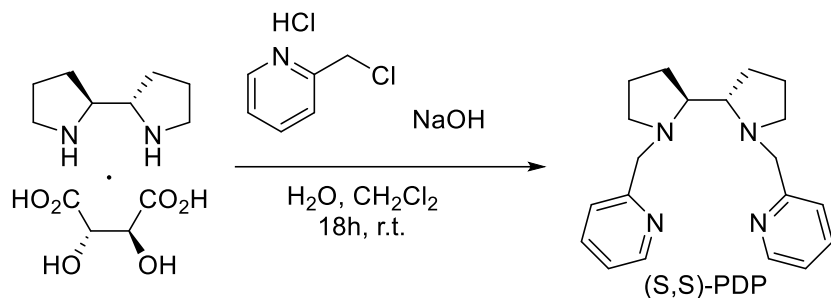
Entry	Product(s)	Yield	RSM	Entry	Product(s)	Yield	RSM
1		45%	40%	3		22%	19%
2		ket-1 25%, ket-2 8%, 15	44%	4		0%	100%

1.3 CONCLUSIONS

Overall, the use of BF₃ as a protecting group for nitrogen functionality successfully allows oxidation in the presence of 1° and 2° amine complexes. While 1° amines are still better suited for the dual-protection strategy (Table 1), we have demonstrated the first successful oxidation of a secondary amine-containing substrate under our standard oxidation conditions. Furthermore, classes such as 3° and aromatic amines remain a challenge for future protection solutions, with the ultimate goal being oxidation of complex alkaloid natural products.

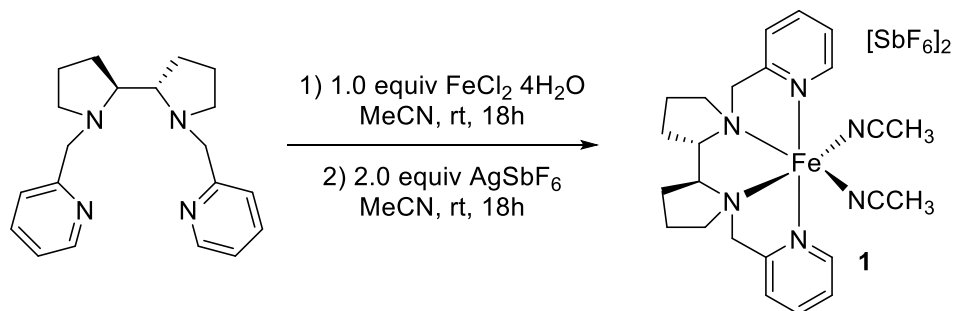
1.4 EXPERIMENTAL SECTION

General Information. The following commercially obtained reagents for the C-H oxidation reaction were used as received: 50% H₂O₂ (Sigma-Aldrich), AcOH (Mallinckrodt), CH₃CN (Sigma-Aldrich). All oxidation reactions were run under air with no precautions taken to exclude moisture. Thin-layer chromatography (TLC) was conducted with E. Merck silica gel 60 F254 precoated plates (0.25 mm) and visualized with UV, potassium permanganate, ceric ammonium molybdate, or Ninhydrin stains. Flash column chromatography was performed using EM reagent silica gel 60 (230-400 mesh). ¹H NMR spectra were recorded on a Varian Unity-500 (500 MHz) narrow bore spectrometer and are reported in ppm using solvent as an internal standard (CDCl₃ at 7.26 ppm). Data reported as: s = singlet, d = doublet, t = triplet, q = quartet, m = multiplet, b = broad, app = apparent; coupling constant(s) in Hz; integration. Proton-decoupled ¹³C-NMR spectra were recorded on a Varian Unity-500 (125 MHz) spectrometer and are reported in ppm using solvent as an internal standard (CDCl₃ at 77.16 ppm).



(-)-2-(((S)-2-((S)-1-(pyridin-2-ylmethyl)pyrrolidin-2-yl)pyrrolidin-1-yl)methyl)pyridine (PDP Ligand). A

200 mL round bottom flask was charged with a stir bar, (S,S)-2,2'-bispyrrolidine tartrate (S2) (1.0 equiv, 4.0 g, 13.8 mmol) and H₂O (30 mL), and CH₂Cl₂ (30 mL). Solid NaOH pellets (6.4 equiv, 3.53 g, 88.2 mmol) were added, followed by 2-picolyl chloride·HCl (2.2 equiv, 4.97 g, 30.3 mmol). After 18 h stirring at room temperature, the reaction mixture was diluted with 1M NaOH. The aqueous layer was extracted with CH₂Cl₂ (3 x 50 mL), and the organic extracts were combined, dried over MgSO₄, and concentrated in vacuo. The crude ligand thus obtained was purified by silica gel chromatography (5% MeOH/2% NH₄OH/CH₂Cl₂) and the collected fractions were combined, washed with 1M NaOH, dried over MgSO₄, and concentrated in vacuo to provide 2.8 g (8.6 mmol) of (S,S')-PDP in 62% isolated yield. ¹H NMR (400 MHz, CDCl₃) δ 8.49 (dd, J = 0.8, 4.8 Hz, 2H), 7.60 (dt, J = 2.0, 7.8 Hz, 2H), 7.39 (d, J = 7.6 Hz, 2H), 7.11 (dd, J = 5.2, 6.0 Hz, 2H), 4.19 (d, J = 14.0 Hz, 2H), 3.49 (d, J = 14.4 Hz, 2H), 2.99 (p, J = 4.4 Hz, 2H), 2.79 (m, 2H), 2.22 (appq, J = 8.4 Hz, 2H), 1.77-1.64 (m, 8H); ¹³C NMR (100 MHz, CDCl₃) δ 160.4, 148.8, 136.3, 122.7, 121.6, 65.3, 61.1, 55.3, 25.9, 23.5; IR (film, cm⁻¹): 2960, 2920, 2872, 2806, 1588, 1570, 1474, 1431, 1366, 1212, 1150, 1120, 1046, 993, 931, 897, 759; HRMS (ESI) m/z calc'd C₂₀H₂₇N₄ [M+H]⁺: 323.2236, found 323.2239; [α]_D²⁵ -94.6° (c 1.0 MeOH).



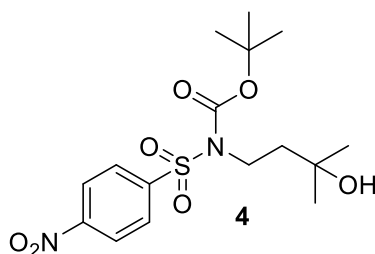
[Fe(S,S-PDP)(CH₃CN)₂](SbF₆)₂ (1)

A 50-mL round bottom flask was charged with (S,S)-PDP ligand (1.095 g, 3.39 mmol, 1 equiv.) and 20 mL CH₃CN. Fe(II)Cl₂·4H₂O (675 mg, 3.39 mmol, 1 equiv) was added to the stirring solution at

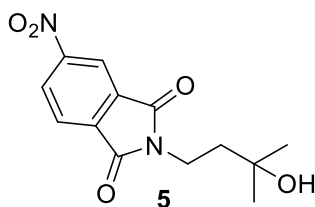
room temperature under a nitrogen atmosphere. Immediately upon adding the Fe source to the (*S,S*)-PDP solution, precipitation of a bright orange solid was observed. Upon stirring for 24 h, diethyl ether was added to the solution to precipitate out the remainder of the complex. The solvent was decanted out of the flask via pipette and the solids were washed thoroughly with ether, and dried under a nitrogen stream for 4 hours to yield Fe(*S,S*PDP)(Cl)₂ (1.29 g, 2.67 mmol, 79% yield): HRMS (ESI) *m/z* calc'd 20H₂₆N₄ClFe [M-Cl]⁺: 413.1195, found 413.1201.

A flame dried 250-mL flask was charged with 608 mg of solid Fe(*S,S*-PDP)(Cl)₂ (1.35 mmol, 1 equiv.) suspended in CH₃CN (17 mL) under nitrogen. Silver hexafluoroantimonate (AgSbF₆, 930 mg, 2.71 mmol, 2 equiv.) was weighed under an inert argon atmosphere and then added to the vigorously stirred heterogeneous mixture. The flask was covered with aluminum foil to protect the silver salts from light. After 16-24 hours, the reaction was filtered through Celite[®] and concentrated under vacuum. The purple solid was redissolved in CH₃CN, filtered through a 0.2 μm Acrodisc[®] LC PVDF filter (HPLC certified), and concentrated. The purple residue was redissolved in CH₃CN and the filtration/concentration procedure was repeated two more times to ensure no silver salts remained. The purple solid obtained was dried under a nitrogen stream for 5 hours to yield [Fe(II)(*S,S*-PDP)(CH₃CN)₂](SbF₆)₂ (**4**) (2.7 g, 3.08 mmol, quantitative yield).

General Procedure A (Iterative Addition Oxidation): A 40 mL screwtop vial was charged with the following: (**R,R**)-**1** (23.3 mg, 0.025 mmol, 5 mol%), *substrate* (0.5 mmol, 1.0 equiv.), CH₃CN (0.75 mL, 0.67 M), and AcOH (15.0 mg, 0.25 mmol, 50 mol%) and a magnetic stir bar. The vial was placed on a stir plate and stirred vigorously at room temperature. A solution of H₂O₂ (50 wt%, 36.8 μL, 0.6 mmol, 1.2 equiv.) in CH₃CN (4.5 mL) was added dropwise via syringe over ca. 45-75 seconds. The first drop of peroxide solution instantly changes the reaction mixture from a reddish-purple color to a dark orange which quickly dissipates to a light yellow/brown. As more peroxide is added, this yellow/brown color slowly changes to a darker amber color. **Significant decreases in yield were noted when the peroxide solution was added rapidly.** No significant difference in yield was noted if the dropwise addition exceeded 75 seconds (up to 150 seconds). After ca. 10 minutes, a solution of **1** (23.3 mg, 0.025 mmol, 5 mol%), AcOH (15 mg, 0.25 mmol, 50 mol%), in CH₃CN (0.5 mL) was added via pipette. This was followed by H₂O₂ (50 wt%, 36.8 μL, 0.6 mmol, 1.2 equiv.) in CH₃CN (4.5 mL) added dropwise over ca. 45-75 seconds. A third addition was done in the same manner for a total of 15 mol%, 1.5 equiv. AcOH, and 3.6 equiv. H₂O₂. Each addition was allowed to stir for 10 minutes, for a total reaction time of 30 minutes.

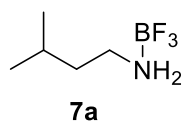


Tert-butyl (3-hydroxy-3-methylbutyl)((4-nitrophenyl)sulfonyl)carbamate (4). Synthesis of compound (4) was achieved via General Procedure A (above). Reaction was concentrated and taken up in minimal dichloromethane, then purified via flash column chromatography to afford the title compound in 55% overall yield. ^1H NMR (500 MHz, Chloroform- d) δ 8.4 (d, J = 8.8 Hz, 2H), 8.1 (d, J = 8.8 Hz, 2H), 4.1 – 3.9 (m, 2H), 2.0 – 1.9 (m, 2H), 1.4 (s, 9H), 1.3 (s, 6H).

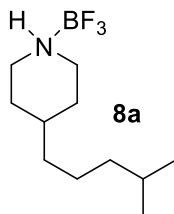


2-(3-hydroxy-3-methylbutyl)-5-nitroisindoline-1,3-dione (5). Synthesis of compound (5) was achieved via General Procedure A (above). Reaction was concentrated and taken up in minimal dichloromethane, then purified via flash column chromatography to afford the title compound in 57% overall yield. ^1H NMR (500 MHz, Chloroform- d) δ 8.7 – 8.6 (m, 1H), 8.6 – 8.6 (m, 1H), 8.6 (dd, J = 8.1, 2.0 Hz, 1H), 8.1 – 8.0 (m, 1H), 4.0 – 3.9 (m, 2H), 1.9 – 1.8 (m, 2H), 1.3 (s, 6H), 8.6 – 8.6 (m, 1H).

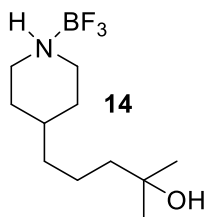
General Procedure B (N- BF_3 protection). To a flame-dried round-bottom flask with a teflon stir bar was added *substrate* (1.0 equivalents), and diluted with dry THF (from SDS, 1M). The solution was cooled to -78°C and Boron Trifluoride Diethyl Etherate ($\text{BF}_3\text{-OEt}_2$, 1.1 equivalents) was added dropwise. The reaction was warmed to 0°C and stirred for 30min-1 hour, monitoring by Thin Layer Chromatography until complete consumption of the substrate was achieved. In some cases, an excess of $\text{BF}_3\text{-OEt}_2$ was added (in 0.2 equivalent successive proportions) to achieve full conversion. Upon completion, the reaction was concentrated down to dryness. Purification was achieved by either recrystallization from appropriate solvent mixtures, or in some cases via flash column chromatography (although some N- BF_3 complexes were not stable to Silica gel).



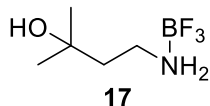
N-(trifluoroboron)-3-methylbutan-1-amine (7a). N-BF₃ complex **7a** was synthesized via **General Procedure B**. Purification was achieved via plugging the crude reaction over silica gel (1 x 3in plug, 100% Ethyl Acetate eluent, ~100mL) to yield the product as a white solid in 93% yield. ¹H NMR (500 MHz, Chloroform-d) δ 3.9 (s, 2H), 3.0 – 2.9 (m, 2H), 1.7 (dt, J = 13.3, 6.7 Hz, 1H), 1.5 (q, J = 7.4 Hz, 2H), 0.9 (d, J = 6.6 Hz, 6H).



N-(trifluoroboron)-4-(4-methylpentyl)piperidine (8a). N-BF₃ complex **8a** was synthesized via **General Procedure B**. Purification was achieved via plugging the crude reaction over silica gel (1 x 3in plug, Ethyl Acetate eluent, ~100mL) to yield the product as a white solid in 94% yield. ¹H NMR (500 MHz, Chloroform-d) δ 3.8 (s, 1H), 3.4 – 3.4 (m, 2H), 2.8 – 2.6 (m, 2H), 1.9 (d, J = 14.1 Hz, 3H), 1.6 – 1.4 (m, 1H), 1.5 – 1.4 (m, 1H), 1.3 – 1.2 (m, 4H), 1.2 (ddd, J = 10.0, 6.8, 3.1 Hz, 3H), 0.9 (d, J = 6.6 Hz, 6H).



N-(trifluoroboron)-2-methyl-5-(piperidin-4-yl)pentan-2-ol (14). Hydroxylation of compound **8a** was achieved via **General Procedure A** (on a 0.2mmol scale). The crude reaction was concentrated and purified via silica gel chromatography (4% MeOH in DCM eluent) to afford 21mg (44%) of **14** as a white solid. ¹H NMR (500 MHz, Chloroform-d) δ 3.8 (s, 1H), 3.4 (d, J = 13.2 Hz, 2H), 2.7 (q, J = 12.1 Hz, 2H), 2.0 – 1.9 (m, 3H), 1.5 – 1.4 (m, 3H), 1.4 – 1.3 (m, 2H), 1.2 (d, J = 15.5 Hz, 9H).



N-(trifluoroboron)-4-amino-2-methylbutan-2-ol (17). Hydroxylation of compound **7a** was achieved via **General Procedure A** (on a 0.2mmol scale). The crude reaction was concentrated and purified via silica gel chromatography (2% to 4% MeOH in DCM eluent) to afford 7mg (22%) of **17** as a white solid. ¹H NMR (500 MHz, Chloroform-d) δ 4.8 (s, 2H), 3.2 (s, 2H), 1.8 – 1.7 (m, 2H), 1.3 (s, 6H).

1.5 REFERENCES

-
- ¹ (a) Dick, A. R.; Sanford, M. S. *Tetrahedron*, **2006**, *62*, 2439-2463. (b) Young, A.J.; White, M.C. *J. Am. Chem. Soc.*, **2008**, *130*, 14090-14091. (c) Chen, M.S.; White, M.C. *Science*, **2007**, *318*, 783-787. (d) Hartwig, J.F.; et.al, *J. Am. Chem. Soc.*, **2006**, *128*, 13684-13685.
- ² "National Library of Medicine", *National Institutes of Health*, <<http://www.nlm.nih.gov/>>.
- ³ Chen, M.S.; White, M.C. *Science*, **2007**, *318*, 783-787.
- ⁴ Tang, K. X.; Guo, B. H.; Kai, G. Y.; Jin, H. B. *Afr. J. Biotechnol.* 2006, *5*, 15-20.
- ⁵ Kim, Y. J.; Man, Kim, N. S.; Patil, P. S.; Ahn, K. D.; Kim, J.; and Kim, T. H. *J. Applied Polymer Science*, **2009**, *111*, 1878-1883.
- ⁶ Hutchins, R. O.; Dux, F. J. *J. Org. Chem*, **1973**, *38*, 1961-2.
- ⁷ (a) Smith, C. H. *Modern Plastics* **1969**, *46*, 118. (b) Chabanne, P. et. Al., *J. App. Pol. Sci.* **1993**, *49*, 685. (c) Contreras, R., et. Al. *Mag. Res. In Chem.*, **1993**, *31*, 189. (d) *Inorg. Chem.* 2001, *40*, 3243.
- ⁸ Burke, M. et. Al., *J. Am. Chem. Soc.* **2007**, *129*, 6716.

CHAPTER 2

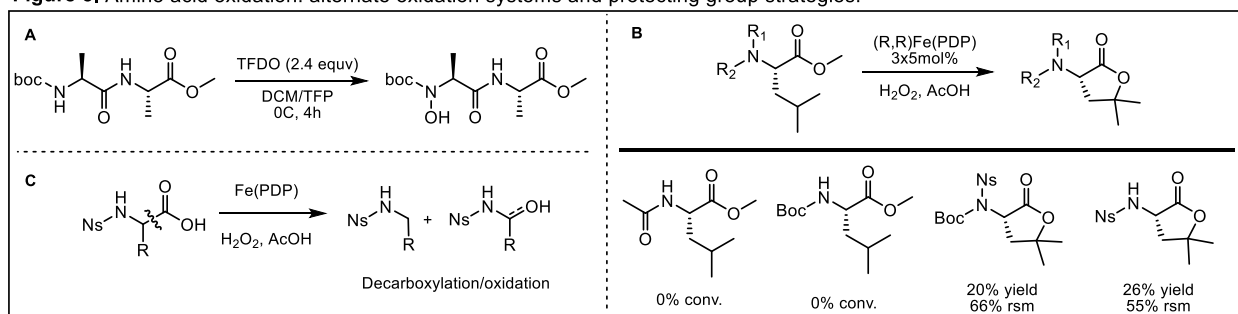
APPLICATION TOWARDS AMINO ACID AND PEPTIDE OXIDATION, WITH FOCUS ON REACTIVITY AND SELECTIVITY TRENDS

2.1 INTRODUCTION

Use of peptides in the pharmaceutical industry has greatly increased in recent years. As of 2005, there were 40 marketed peptides worldwide, 270 in clinical phase testing, and over 400 in advanced pre-clinical trials. Peptides have many advantages over small molecule drug treatments such as high activity and target specificity, minimal drug-drug interactions, low tissue accumulation, and high biological/chemical diversity¹. However many limitations also remain, low oral availability (must dose via injection), low biological stability, solubility and biological clearing problems, and ultimately challenging and costly syntheses¹. The high promise of peptides as pharmaceutical agents has led our group to be interested in developing methods to simplify the synthetic process via direct oxidation and subsequent diversification using our non-heme iron oxidation methodology.

Utilizing principles from our efforts towards nitrogen tolerance for our non-heme iron catalyst, we began to evaluate direct oxidation of amino acids and small peptides, the major challenge being dense functionality, of which Nitrogen moieties are a primary concern. All amino acids contain amine and carboxylic acid backbones, with a variety of other functionality depending on the side-chain substituents. In the context of small peptides, we were also aware of the possibility of amide oxidation to the corresponding N-oxides, a prevalent oxidative pathway with small molecule oxidants such as dimethyldioxirane (DMDO) and trifluoromethyldioxirane (TFDO)² (Figure 5, A). Other metal-based methods have been developed in the Sames group to effect similar amino-acid aliphatic oxidations using platinum³, however substrate scope is highly limited, and selectivities and overall yields are less than synthetically useful.

Figure 5. Amino acid oxidation: alternate oxidation systems and protecting group strategies.



2.2 RESULTS AND DISCUSSION

Optimization of backbone (amine and carboxylic acid) protecting groups was first evaluated. Starting with Leucine methyl ester, several common N-protecting groups were tested under the standard oxidation conditions for product conversion. When either an N-acetyl or N-Boc group was appended, no conversion was observed whatsoever (Figure 5, B). We then attempted a dual protection strategy using the N-Boc-N-Nosyl variant, which yielded 20% of the desired lactone. Due to its highly electron-withdrawing nature, we attempted the mono-protected N-nosyl leucine, which not only underwent productive oxidation, but produced an increased lactone yield of 26% with 55% recovered starting material. Although previously a single nosyl group was not sufficient to allow productive oxidation (Table 1, entry 2), we hypothesize that the electron-withdrawing nature of the adjacent ester moiety decreased electron density at Nitrogen enough to prevent catalyst binding. At the C-terminus, we were aware that carboxylic acids act as directing groups for oxidation. We then tested the necessity of the C-terminal ester group. To our surprise, the N-nosyl amino acid readily decarboxylated under the standard oxidation conditions (Figure 5, C). (Although the mechanism of this decomposition is currently unknown, small amounts of α -oxidation suggest that oxidation occurs first at the α -C-H bond, which promotes decarboxylation). From these studies, N-nosyl amino esters were selected as the standard motif for amino acid and peptide protection during non-heme oxidation.

With a general protection strategy developed, we focused on single amino acid oxidation, first assessing which residues are stable to the oxidation conditions (Table 4). The methyl esters of both Aspartic and Glutamic Acid (**19** and **20**) were both re-isolated in >95% (entries 1 and 2). In the case of Serine and Threonine, acetate protection of the free alcohol afforded stable compounds, as >95% of both **21** and **22** were recovered (entries 3 and 4). Lysine is a special case in that it has an amine-containing side-chain as well as the α -amine. Considering the ϵ -amine (side chain) does not benefit from the electron withdrawing properties of the ester, it was necessary to use the dual protection strategy discussed above. In order to avoid lengthy orthogonal protection strategies, bis-4-nitrophthalimide methyl ester **33** was tested, and recovered in 90% after oxidation (entry 5). Considering BF_3 protection was best utilized with cyclic, 2° amines, Proline was complexed and tested. Not surprisingly from our results above, Proline Methyl Ester- BF_3 complex **24** was recovered in >95% after oxidation (entry 6). Entries 7-10 show several derivatives of Phenylalanine with varying electron-withdrawing substitution. Protected difluorophenylalanine **25** was only recovered in 37% yield after oxidation, with the remainder of the mass balance going to unproductive and unisolable oxidation of the

phenyl ring (entry 7). The tri-fluorinated variant, **26**, showed a drastic improvement, with 77% recovered after oxidation (entry 8). Although this number is low compared to entries 1-6, our hope is that the catalyst will select for more reactive C-H bonds of other residues when in the context of a small peptide (see below). Although Fluorine is inductively electron withdrawing, it can also donate electron density via its lone pairs. This is not the case, however, with nitro and trifluoromethyl groups, both of which are highly electron withdrawing substituents. It is not surprising, then, that *p*-nitrophenylalanine **27** and 3,5-bistrifluoromethylphenylalanine **28** were both recovered in >95% after oxidation (entries 9 and 10).

Table 4. Oxidatively stable single Amino Acids, natural and unnatural residues.

$\text{PG-NH-CH(R)-COOMe} \xrightarrow[\text{H}_2\text{O}_2, \text{AcOH}]{(\text{R,R})\text{Fe}(\text{PDP}) \text{ 3 x 5\%}} \text{PG-NH-CH(R)-COOMe}$											
Entry	Substrate	rsm	Entry	Substrate	rsm	Entry	Substrate	rsm	Entry	Substrate	rsm
1 2		n=1, 19 >95% n=2, 20 >95%	5		90%	7		37%	9		>95%
3 4		R=H, 21 >95% R=Me, 22 >95%	6		>95%	8		77%	10		>95%

Next we sought to apply our methodology to natural amino acids with oxidizable functionality (Table 5). Under slow addition (syringe pump) conditions, with elevated levels of hydrogen peroxide and acetic acid (9.0 and 1.0 equivalents, respectively) as optimized conditions, Leucine methyl ester **29** was oxidized to the corresponding lactone in 44% yield, with 25% recovered starting material (entry 1). Use of the *tert*-butyl ester at the C-terminus of Leucine (37) prevents spontaneous lactonization, and the free alcohol was isolated in 48% yield with 24% recovered starting material (entry 2). Valine methyl ester **30** undergoes oxidation in a similar fashion, yielding the free alcohol in 39% yield and 45% recovered starting material (entry 3). In this case, formation of the 4-membered lactone is disfavored, and use of the *t*Butyl ester was not necessary. As expected, Valine suffers from slightly lower reactivity than Leucine, a consequence of the proximity to the electron-withdrawing backbone resulting in a more electron-deficient C-H bond. The mass balance for oxidation of Valine is significantly higher than that of

Leucine as well, suggesting the isobutyl side chain of Leucine undergoes alternate or over oxidation not possible for the isopropyl moiety of Valine.

Table 5. Oxidatively susceptible natural amino acid residues.

$\text{PG-NH-CH(R)-COOMe} \xrightarrow[\text{H}_2\text{O}_2, \text{AcOH}]{(\text{R,R})\text{Fe(PDP)}} \text{PG-NH-CH(R-OH)-COOMe}$									
Entry	Substrate	Product	SM	Yield	Entry	Substrate	Product	SM	Yield
1 ^a			25%	44%	3 ^a			45%	39%
2 ^a			24%	48%					

a) 25mol% catalyst, slow addition. 9.0 equiv H₂O₂, 1.0equiv AcOH.

In recent years, there has been an increased interest in unnatural amino acid production and incorporation into pharmaceutical peptides. Work by the Schulz group^x provoked an interest in a variety of linear aliphatic amino acids, with carbon chains ranging from 3-6 atoms long. With multiple sites of potential oxidation available, selectivity becomes an important issue. The sterics and electronics of the backbone were modified in an effort to influence the selectivity to produce a single ketone product in synthetically useful yields. We first looked at n-Hexylglycine with a variety of protecting group combinations (Table 6, entries 1-4). Under standard protection as the N-Nosyl Methyl ester, slow addition protocol afforded 19% of methyl ketone **33**, while ketone formation at carbons 2 and 3 were isolated in similar yields to give an overall product distribution of 1.6 : 1.6 : 1 (entry 1). The *t*Butyl ester (increased sterics) did not improve the yield of **34** (19%), however a small increase in selectivity was observed (1.9 : 1.5 : 1) (entry 2). Addition of a second electron withdrawing group to the amine (N-Nosyl-N-Boc methyl ester) afforded **35** in a slightly increased yield of 22% while maintaining similar selectivities (1.8 : 1.4 : 1) (entry 3). A combination of the dual protection with the *t*Butyl ester, somewhat surprisingly, yielded **36** in 19% yield and low selectivity of 1.6 : 1.4 : 1 (entry 4). Shorter chains were also assessed. N-Nosyl Norvaline methyl ester, under slow addition protocol, afforded ketone **37** in 17% yield, with 65% recovered starting material and no other isolable products (entry 5). Using elevated oxidant this yield could be optimized to 22% (entry 6). Extension of the carbon chain to 4 (Norleucine) afforded ketone **38** in a substantially higher yield of 35%, with 45% of the starting material

recovered (entry 7). This was then re-subjected to the reaction conditions, and a combined yield of 44% of ketone **38** was obtained (entry 8). Although elevated oxidant was used (entry 9), yield of the desired ketone did not increase (35%), and the overall mass balance was much lower with only 26% of the starting material recovered (entry 9).

Table 6. Oxidatively susceptible unnatural Amino Acid residues.

Entry	Substrate	Major Product	SM	Yield	Selectivity (1 : 2 : 3)	
1 ^a			R1= Ns, R2=H, R3=Me, 33	28%	19%	1.6:1.6:1
2 ^a			R1= Ns, R2=H, R3=tBu, 34	27%	19%	1.9:1.5:1
3 ^a			R1= Ns, R2=Boc, R3=Me, 35	25%	22%	1.8:1.4:1
4 ^a			R1= Ns, R2=Boc, R3=tBu, 36	25%	19%	1.6:1.4:1
5 ^a				65%	17%	--
6 ^b				52%	22%	--
7 ^a				45%	35%	~6:1
8 ^a				(23%) ^c	(44%) ^c	--
9 ^b				26%	35%	--

a) 5.5 equiv H₂O₂, 0.5 equiv AcOH. b) Elevated conditions: 9equiv H₂O₂, 1.0 equiv AcOH. c) recovered starting material was resubjected to the reaction conditions, and product yields were combined.

Oxidation of amino acid residues in the context of dipeptides was also explored. Combinations of Leucine or Valine with oxidatively stable residues were synthesized and tested under standard reaction conditions (Table 7). Oxidation of Valine-Glutamic Acid dipeptides show increased reactivity with Valine at the N-terminus (**39**, 41% yield) versus the C-terminus (**43**, 18% yield) (entries 1 and 2). Although less dramatic, this trend held true for Leucine-Glutamic Acid dipeptides, affording **40** in 28% yield and **44** in 24% yield (entries 3 and 4). An interesting feature of the Leucine-containing peptides is the markedly decreased reactivity in the context of a dipeptide versus that of the single amino acid oxidation. Yields for N-terminal Valine (41%) match the result of mono-Valine oxidation, as expected (39%, table 5, entry 3). While oxidation of mono-Leucine affords 44-48% of the oxidized product (Table 5, entry 1 and 2), yield of N-terminal Leucine oxidation in a peptide was significantly lower. To assess whether Glutamic Acid was imparting electronic or steric hindrance of Leucine oxidation, we synthesized and tested the Alanine-containing analogs of each dipeptide in an effort to eliminate these effects with a

smaller, neutral side chain (entries 5-8). Once again, N-terminal Valine was oxidized to **41** in a 42% yield, comparable to the single amino acid (39% yield), while C-terminal Valine remained less reactive, affording **45** in a 20% yield (entries 5 and 6). Low reactivity for Leucine at the N-terminus continued to be problematic, affording **42** in 25% yield (entry 7), with the C-terminal residue yielding 20% of **46** (entry 8). These results rule out Glutamic Acid as the problem for low reactivity of Leucine in a peptide setting, and further studies will be required to determine the cause of differing reactivity.

Table 7. Dipeptide oxidation: oxidizable vs. oxidatively stable residues.

Entry	Product	SM	Yield	Entry	Product	SM	Yield
1		19%	41%	2		49%	18%
3		44%	28%	4		40%	24%
5		15%	42%	6		25%	20%
7		37%	25%	8		37%	20%

Competition studies were also conducted in a dipeptide setting to determine selectivity between two oxidizable residues, noting differences in selectivity for oxidation at the C- vs. N-termini (Table 8). Entry 1, oxidation of a Valine-Valine dipeptide, shows a clear preference for oxidation at the N-terminal residue, yielding 37% of the mono-hydroxylated product and 51% of the unoxidized starting material recovered. The remaining material was isolated as a mixture of C-terminal hydroxylation and di-hydroxylation products (inseparable via chromatography), in a combined yield of 12%. Hydroxylation at the C-terminus could be completely prevented by using the *tert*-butyl ester analog, however overall

reactivity was drastically decreased (entry 2). While no C-terminal oxidation or di-hydroxylation products were observed, the N-terminal hydroxylated product was only produced in a 14% yield, with 71% of the unoxidized starting material recovered. This increase in selectivity can be attributed to increased steric bulk of the *tert*-butyl ester group. The decreased overall reactivity, however, is less straightforward. We hypothesize that *tert*-butyl esters may not be compatible with the Lewis-acidic nature of the catalyst (currently under further investigation). In the case of a Leucine-Leucine dipeptide, N-terminal residue preference was less dramatic, although still apparent. Oxidation at the N-terminal residue yielded 27% hydroxylation product, while a mixture of C-terminal and di-hydroxylated products were isolated in less than 20% yield, with 47% of unoxidized starting material recovered (entry 3). In this case, the *tert*-butyl ester was used to prevent lactonization of the C-terminal hydroxylated product (a spontaneous process that occurs when the methyl-ester analog is used). This was done to provide isolation of the hydroxyl-product for direct comparison to the N-terminal residue, as well as to promote an increased selectivity for oxidation at the N-terminal residue by increased steric bulk at the C-terminus. While the yield of the N-terminal product was less than that of the Valine-Valine analog, the overall mass balance was similarly high. The decreased yield, then, can be attributed to the decrease in selectivity. We hypothesize that this is due to the increased distance of the reactive methine proton from the steric and electronic influence of the peptide backbone for the Leucine side chain versus that of a Valine.

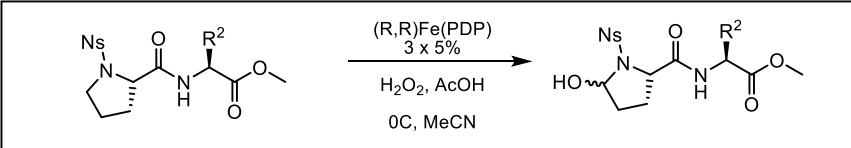
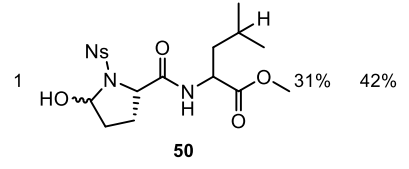
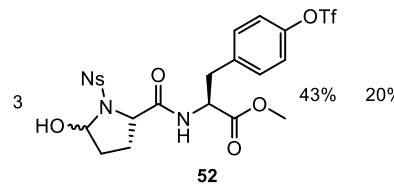
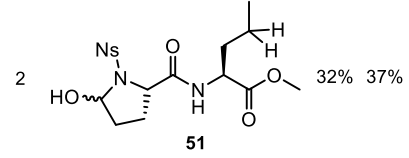
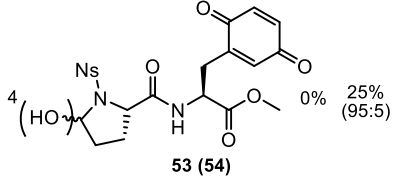
Table 8. Dipeptide oxidation: oxidizable vs. oxidizable residues.

Entry	Product	SM	Yield	Entry	Product	SM	Yield
1	 $R' = \text{OH}, R'' = \text{H}$, 47 $R' = \text{H}, R'' = \text{OH}$ $R' = \text{OH}, R'' = \text{OH}$	51%	37% 12% ^a	3	 $R' = \text{OH}, R'' = \text{H}$, 49 $R' = \text{H}, R'' = \text{OH}$ $R' = \text{OH}, R'' = \text{OH}$	47%	27% <20% ^a
2	 $R' = \text{OH}, R'' = \text{H}$, 48 $R' = \text{H}, R'' = \text{OH}$ $R' = \text{OH}, R'' = \text{OH}$	76%	14% 0% ^a				

Note: Standard Slow Addition protocol used in each oxidation. a) products were isolated as a mixture and yield determined based on 1H NMR ratios.

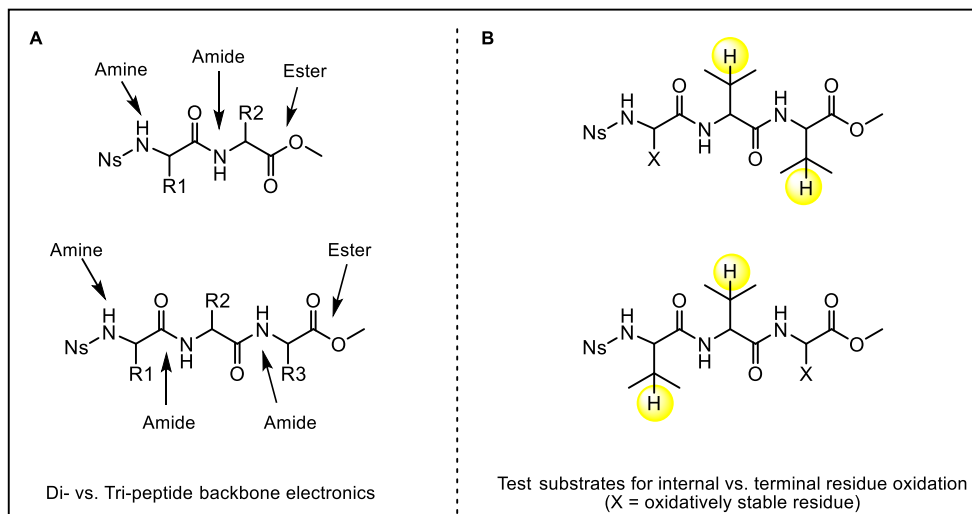
Next we looked at Proline, which was found to have unique reactivity under the oxidation conditions (to form the hemiaminal). We continued our competition studies by synthesizing several dipeptides with Proline at the N-terminus, and another oxidizable residue at the C-terminus (Table 9). To our delight, we saw high selectivity for Proline oxidation in the presence of known oxidizable residues, however overall yields were not optimal. In entries 1 and 2, an aliphatic residue was placed at the C-terminus. In the case of Proline-Leucine, hemiaminal **50** was formed in 42% yield and 31% recovered starting material, with no oxidation at Leucine observed (entry 1). For nor-Valine (containing a methylene active site, entry 2), oxidation to hemiaminal **51** was achieved in 37%, with 31% recovered starting material and no observed oxidation of the aliphatic side-chain. We then turned our attention to aromatic-containing residues, which are typically incompatible with the oxidative conditions unless highly electron deficient. A triflate-protected Tyrosine residue survived and yielded hemiaminal **52** in a slightly-decreased 20% yield with 43% recovered starting material (entry 3). This is not surprising, as the aryl group is only slightly electron-deficient; yet still proving that oxidation to the hemiaminal is a highly favorable process. When the aryl group is neutral, however, as in the case of a Phenylalanine residue, the majority of the material is converted to the quinone analog **53** by aryl oxidation (entry 4). This material was isolated as a mixture of the quinone and hemiaminal-quinone **54** (di-oxidized product) in a 25% yield, in a 95:5 ratio. Therefore only about 1% of the overall process produced hemiaminal product, and oxidation to the hemiaminal was only effected after the quinone was formed. From this we see that although hemiaminal formation is a favorable process, oxidation of electron-rich aryls will still occur selectively under the reaction conditions. Further studies will also need to be conducted, if possible, to improve the reactivity of these proline dipeptides in order to achieve synthetic utility.

Table 9. Dipeptide oxidation: selective proline oxidation.

							
Entry	Product	SM	Yield	Entry	Product	SM	Yield
1		31%	42%	3		43%	20%
2		32%	37%	4		0%	25% (95:5)

On the subject of oxidative selectivity within a peptide moiety, further studies are ongoing in our group. At this point, only dipeptide structures have been tested for selectivity, differentiating exclusively between the C- and N- termini. However, in longer peptide structures, internal residues are flanked by two amide moieties, as opposed to an amine and amide (N-terminus) or an amide and an ester (C-terminus), overall leading to a third electronic environment (Figure 6, A). A series of tripeptide oxidation studies will need to be conducted in order to flesh out full selectivity rules for longer peptide chain oxidations. To test this, tripeptides will be synthesized that contain a terminal and internal oxidatively susceptible residue, with the alternate terminus containing an oxidatively stable residue (Figure 6, B). By comparing a single terminus to a single internal residue and using 2 separate tripeptides, we can simplify purification of oxidation product mixtures while still obtaining useful selectivity information.

Figure 6. Future tripeptide oxidation selectivity studies.



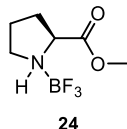
2.3 CONCLUSIONS

Reactivity and selectivity trends among various amino-acid residues were explored as both single amino-acids and multi-residue small peptides. Amino acids were grouped based on oxidative susceptibility and oxidative stability, with protecting group schemes for incompatible side-chain motifs being developed to allow for productive oxidation. Selectivity studies within a dipeptide motif were then conducted, assessing trends such as (1) relative head-to-head reactivity between various residues, (2) relative reactivity based on location within a peptide setting, and (3) relative selectivity trends of various sites within a single residue. Distinct evidence was found to favor oxidation at the N-terminus preferentially to that of the C-terminus, while highly activated Aryl and Aza-cyclic moieties were found to be much more reactive than electron-poor (non-reactive) or aliphatic (moderately reactive) side chains. Interestingly, reactivity trends sometimes differed between a single-residue setting and within the context of a peptide, such as the case for Leucine, while other times this disparity was not apparent (as with Valine). Other anomalies include the highly reactive Proline residue, favoring hemiaminal formation that is not prevalent in the analogous pyrrolidine motif.

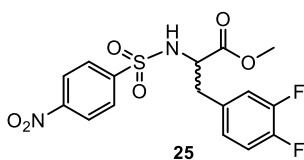
2.4 EXPERIMENTAL SECTION

General Information. The following commercially obtained reagents for the C-H oxidation reaction were used as received: 50% H₂O₂ (Sigma-Aldrich), AcOH (Mallinckrodt), CH₃CN (Sigma-Aldrich). All oxidation reactions were run under air with no precautions taken to exclude moisture. Thin-layer chromatography (TLC) was conducted with E. Merck silica gel 60 F254 precoated plates (0.25 mm) and visualized with UV, potassium permanganate, ceric ammonium molybdate, or Ninhydrin stains. Flash column chromatography was performed using EM reagent silica gel 60 (230-400 mesh). ¹H NMR spectra were recorded on a Varian Unity-500 (500 MHz) narrow bore spectrometer and are reported in ppm using solvent as an internal standard (CDCl₃ at 7.26 ppm). Data reported as: s = singlet, d = doublet, t = triplet, q = quartet, m = multiplet, b = broad, app = apparent; coupling constant(s) in Hz; integration. Proton-decoupled ¹³C-NMR spectra were recorded on a Varian Unity-500 (125 MHz) spectrometer and are reported in ppm using solvent as an internal standard (CDCl₃ at 77.16 ppm).

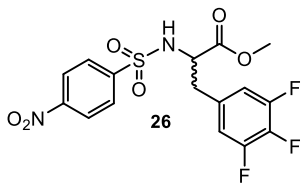
General Procedure C (Iron C-H Oxidation Slow Addition Protocol). 25 mol% catalyst **1**: A 40 mL screwtop vial was charged with the following: substrate (0.5 mmol, 1.0 equiv), CH₃CN (1.0 mL, 0.5 M), and AcOH (15.0 mg, 0.25 mmol, 0.5 equiv) and a magnetic stir bar. The vial was placed on a stir plate and stirred vigorously at room temperature while open to ambient atmosphere. A 1.0 mL glass syringe was charged with a solution of Fe(PDP) **1** catalyst (116.5 mg, 0.125 mmol, 25 mol %) in CH₃CN (0.625 mL, 0.2 M) and loaded into a syringe pump set with an addition rate of 0.5 mL/1 h (0.0083 mL/min). A 10 mL glass syringe was charged with a solution of H₂O₂ (50 wt % in H₂O, 170 μL, 2.5 mmol, 5.0 equiv) in CH₃CN (6.25 mL, 0.4 M) and loaded into a syringe pump set with an addition rate of 5 mL/1 h (0.083 mL/min). Both syringes were equipped with 26G needles and directed into the center of the uncapped vial; precautions should be taken not to touch the sides. The two additions were initiated simultaneously and both Fe(PDP) **1** catalyst and H₂O₂ were added to the reaction vial over the course of 75 min. The crude mixture was concentrated via rotary evaporation to a minimal amount of CH₃CN and taken up in ethyl acetate. Dry Silica was added, and the crude reaction was concentrated to dryness (adsorbed onto the silica gel) and purified by flash chromatography.



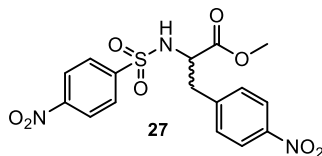
(S)-N-(trifluoroboron)-Proline-Methyl Ester (24). N-protected Proline (24) was synthesized via **General Procedure B** and subjected to the iterative addition oxidation (general procedure A). Post-oxidation, the reaction was purified via flash column chromatography to yield >95% of recovered starting material. ¹H NMR (500 MHz, Acetonitrile-d₃) δ 5.7 (s, 1H), 4.1 – 4.0 (m, 1H), 3.8 (s, 3H), 3.3 (dd, J = 11.7, 6.0 Hz, 1H), 3.1 – 3.0 (m, 1H), 2.3 (dt, J = 13.8, 7.9 Hz, 1H), 2.0 (td, J = 15.7, 7.0 Hz, 2H), 1.8 (dd, J = 14.0, 6.9 Hz, 1H).



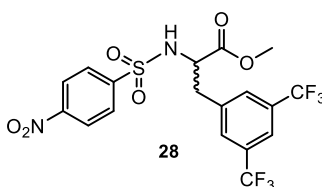
Methyl 3-(3,4-difluorophenyl)-2-((4-nitrophenyl)sulfonamido)propanoate (25). Compound **25** was subjected to **General Procedure A**. The crude reaction was concentrated and purified via flash column chromatography yielding 37% of the starting material recovered, with loss of 63% of the remaining mass balance. ¹H NMR (500 MHz, Chloroform-d) δ 8.4 – 8.2 (m, 2H), 8.0 – 7.8 (m, 2H), 7.0 (dt, J = 10.3, 8.2 Hz, 1H), 6.9 (ddd, J = 10.3, 7.3, 2.3 Hz, 1H), 6.9 – 6.8 (m, 1H), 5.4 (d, J = 8.8 Hz, 1H), 4.2 (ddd, J = 8.9, 6.2, 4.9 Hz, 1H), 3.6 (s, 3H), 3.1 (dd, J = 14.0, 5.4 Hz, 1H), 3.0 (dd, J = 14.0, 6.7 Hz, 1H).



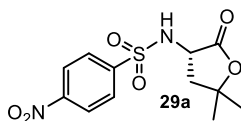
Methyl 2-((4-nitrophenyl)sulfonamido)-3-(3,4,5-trifluorophenyl)propanoate (26). Compound **26** was subjected to **General Procedure A**. The crude reaction was concentrated and purified via flash column chromatography yielding 77% of the starting material recovered, with loss of 23% of the remaining mass balance. ¹H NMR (500 MHz, Acetonitrile-d₃) δ 8.3 (d, J = 8.9 Hz, 2H), 7.9 (d, J = 8.9 Hz, 2H), 6.9 (dd, J = 9.0, 6.6 Hz, 2H), 6.5 – 6.4 (m, 1H), 4.2 (td, J = 9.4, 4.7 Hz, 1H), 3.6 (s, 3H), 3.1 (dd, J = 14.2, 4.6 Hz, 1H), 2.8 (dd, J = 14.2, 9.8 Hz, 1H).



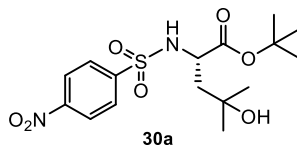
Methyl 3-(4-nitrophenyl)-2-((4-nitrophenyl)sulfonamido)propanoate (27). Compound **27** was subjected to **General Procedure A**. The crude reaction was concentrated and purified via flash column chromatography yielding >95% of the starting material recovered. ^1H NMR (499 MHz, Acetonitrile- d_3) δ 8.2 (d, J = 8.9 Hz, 2H), 8.0 (d, J = 8.7 Hz, 2H), 7.8 (d, J = 8.9 Hz, 2H), 7.3 (d, J = 8.7 Hz, 2H), 6.5 (d, J = 9.7 Hz, 1H), 4.3 (q, J = 5.0 Hz, 1H), 3.6 (s, 3H), 3.2 (dd, J = 14.0, 4.9 Hz, 1H), 3.0 (dd, J = 14.0, 10.0 Hz, 1H).



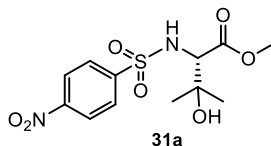
Methyl 3-(3,5-bis(trifluoromethyl)phenyl)-2-((4-nitrophenyl)sulfonamido)propanoate (28). Compound **28** was subjected to **General Procedure A**. The crude reaction was concentrated and purified via flash column chromatography yielding >95% of the starting material recovered. ^1H NMR (500 MHz, Acetonitrile- d_3) δ 8.2 (d, J = 8.9 Hz, 2H), 7.8 (d, J = 8.9 Hz, 3H), 7.8 (s, 2H), 6.5 (d, J = 9.6 Hz, 1H), 4.3 (td, J = 9.8, 4.8 Hz, 1H), 3.6 (s, 3H), 3.3 (dd, J = 14.1, 4.7 Hz, 1H), 3.0 (dd, J = 14.1, 10.0 Hz, 1H).



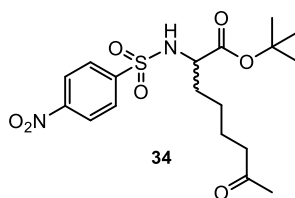
(S)-N-(5,5-dimethyl-2-oxotetrahydrofuran-3-yl)-4-nitrobenzenesulfonamide (29a). Compound **29** was subjected to **General Procedure C** (Slow Addition oxidation). The crude reaction was concentrated and purified via silica gel chromatography to yield the title compound as a white solid in 44% yield, with 25% of the starting material recovered. ^1H NMR (500 MHz, Chloroform- d) δ 8.39 (d, J = 8.7 Hz, 2H), 8.13 (d, J = 8.8 Hz, 2H), 5.68 (s, 1H), 4.30 (dd, J = 11.6, 8.7 Hz, 1H), 2.61 (dd, J = 12.8, 8.7 Hz, 1H), 2.04 (t, J = 12.2 Hz, 1H), 1.49 (s, 3H), 1.40 (s, 3H); ^{13}C NMR (126 MHz, Chloroform- d) δ 173.4, 150.5, 145.6, 128.7, 124.7, 83.7, 53.5, 43.0, 29.0, 27.1; IR (film, cm^{-1}) 3302, 3109, 2980, 2939, 1770, 1606, 1531, 1454, 1351, 1308, 1167, 1109, 1093, 922, 854, 739, 687, 617; HRMS (ESI) m/z calc'd for $\text{C}_{12}\text{H}_{14}\text{N}_2\text{O}_6\text{SNa}$ $[\text{M}+\text{Na}]^+$: 337.0470, found 337.0469.



(S)-tert-butyl 4-hydroxy-4-methyl-2-((4-nitrophenyl)sulfonamido)pentanoate (30a). Compound **30** was subjected to **General Procedure C** (Slow Addition oxidation). The crude reaction was concentrated and purified via silica gel chromatography to yield the title compound as a white solid in 48% yield, with 24% of the starting material recovered. ^1H NMR (500 MHz, Chloroform-*d*) δ 8.35 (d, *J* = 8.8 Hz, 2H), 8.08 (d, *J* = 8.7 Hz, 2H), 5.92 (d, *J* = 7.2 Hz, 1H), 4.10 (td, *J* = 7.6, 4.9 Hz, 1H), 1.92 – 1.78 (m, 2H), 1.34 (s, 3H), 1.30 (s, 9H), 1.28 (s, 3H); ^{13}C NMR (126 MHz, Chloroform-*d*) δ 170.9, 150.2, 145.8, 128.9, 124.3, 83.0, 71.2, 54.7, 44.1, 30.7, 29.1, 27.8; IR (film, cm^{-1}) 3535, 3510, 3271, 3109, 2978, 2931, 1732, 1606, 1531, 1350, 1309, 1255, 1153, 1092, 939, 856, 739, 685615; HRMS (ESI) *m/z* calc'd for $\text{C}_{16}\text{H}_{25}\text{N}_2\text{O}_7\text{S}$ [$\text{M}+\text{H}$] $^+$: 389.1382, found 389.1383.

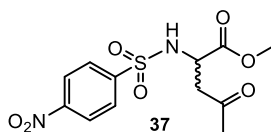


(S)-Methyl 3-hydroxy-3-methyl-2-((4-nitrophenyl)sulfonamido)butanoate (31a). Compound **31** was subjected to **General Procedure C** (slow addition oxidation). The crude reaction was concentrated and purified via silica gel chromatography to yield the title compound as a white solid in 39% yield, with 45% of the starting material recovered. ^1H NMR (500 MHz, Chloroform-*d*) δ 8.35 (d, *J* = 8.8 Hz, 2H), 8.05 (d, *J* = 8.8 Hz, 2H), 6.19 (d, *J* = 10.2 Hz, 1H), 3.85 (d, *J* = 10.2 Hz, 1H), 3.48 (s, 3H), 1.31 (s, 3H), 1.25 (s, 3H); ^{13}C NMR (126 MHz, Chloroform-*d*) δ 171.0, 150.3, 145.7, 128.7, 124.4, 72.1, 63.5, 52.6, 26.9, 26.7; IR (film, cm^{-1}) 3529, 3263, 3107, 2983, 2929, 1736, 1531, 1352, 1314, 1169, 1092, 856, 737, 617; HRMS (ESI) *m/z* calc'd for $\text{C}_{12}\text{H}_{17}\text{N}_2\text{O}_7\text{S}$ [$\text{M}+\text{H}$] $^+$: 333.0756, found 333.0756.

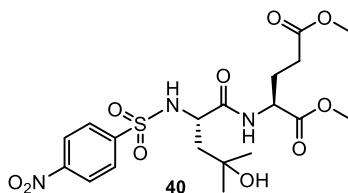


Tert-butyl 2-((4-nitrophenyl)sulfonamido)-7-oxooctanoate (34). The title compound was isolated as a white foam following oxidation using **General Procedure A** (iterative addition protocol). The major

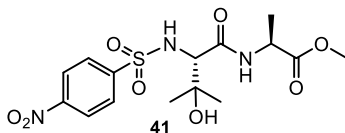
product was isolated via purification using Medium Performance Liquid Chromatography to isolate this specific isomer in 19% overall yield. The product ratio was 1.9 : 1.5 : 1 in favor of the methyl ketone (34) over the ethyl and propyl variants, respectively. ^1H NMR (500 MHz, Chloroform-d) δ 8.3 (d, J = 8.6 Hz, 2H), 8.0 (d, J = 8.6 Hz, 2H), 5.5 (d, J = 9.2 Hz, 1H), 3.9 – 3.8 (m, 1H), 2.4 (t, J = 7.2 Hz, 2H), 2.1 (s, 3H), 1.8 – 1.7 (m, 1H), 1.7 – 1.5 (m, 3H), 1.4 (q, J = 7.5 Hz, 2H), 1.2 (s, 9H).



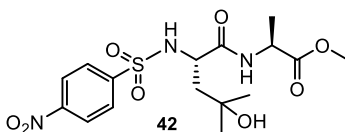
Methyl 2-((4-nitrophenyl)sulfonamido)-4-oxopentanoate (37). The title compound was isolated as a white semi-solid following oxidation using **General Procedure A** (iterative addition protocol). The reaction was purified via flash chromatography on silica to yield the title compound as the only major product in 17% yield, with 65% of the starting material recovered. ^1H NMR (500 MHz, Chloroform-d) δ 8.4 (d, J = 8.8 Hz, 2H), 8.1 (d, J = 8.8 Hz, 2H), 5.8 (d, J = 8.4 Hz, 1H), 4.1 (dt, J = 8.5, 4.1 Hz, 1H), 3.6 (s, 3H), 3.2 (dd, J = 18.4, 4.0 Hz, 1H), 3.1 (dd, J = 18.4, 4.1 Hz, 1H), 2.2 (s, 3H).



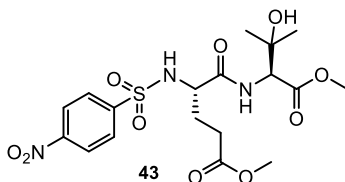
(S,S)-Dimethyl (4-hydroxy-4-methyl-2-((4-nitrophenyl)sulfonamido)pentanoyl)glutamate (40). Parent dipeptide Ns-Leu-Glu(OMe)-OMe was oxidized to the title compound using **General Procedure C** (slow addition protocol) with an elevated oxidant modification: H_2O_2 (9.0 equiv) and Acetic Acid (1.0 equiv). The reaction was concentrated and purified via flash column chromatography on silica gel to afford the title compound as a colorless oil in 28% yield (44% recovered starting material). ^1H NMR (500 MHz, Chloroform-d) δ 8.3 (d, J = 8.8 Hz, 2H), 8.0 (d, J = 8.8 Hz, 2H), 5.5 (d, J = 8.9 Hz, 1H), 4.0 (td, J = 9.2, 4.5 Hz, 1H), 3.5 (s, 3H), 2.7 (ddd, J = 18.6, 8.1, 6.1 Hz, 1H), 2.6 (dt, J = 18.6, 6.1 Hz, 1H), 2.2 (s, 3H), 2.2 – 2.1 (m, 1H), 1.8 (ddt, J = 14.5, 9.5, 6.1 Hz, 1H).



(S,S)-Methyl (3-hydroxy-3-methyl-2-((4-nitrophenyl)sulfonamido)butanoyl)alaninate (41). Parent dipeptide Ns-Val-Ala-OMe was oxidized to the title compound using **General Procedure C** (slow addition protocol) with an elevated oxidant modification using H₂O₂ (9.0 equiv) and Acetic Acid (1.0 equiv). The reaction was concentrated and purified via flash column chromatography on silica gel to afford the title compound as a white solid in 42% yield (15% recovered starting material). ¹H NMR (500 MHz, Chloroform-d) δ 8.3 (d, J = 9.0 Hz, 2H), 8.1 (d, J = 8.8 Hz, 2H), 7.6 – 7.4 (m, 1H), 6.8 (s, 1H), 4.4 (dtd, J = 8.2, 5.2, 2.6 Hz, 1H), 4.0 (d, J = 6.0 Hz, 1H), 3.7 (s, 3H), 3.7 (s, 3H), 2.4 – 2.2 (m, 2H), 2.1 – 2.0 (m, 1H), 1.9 (ddd, J = 6.5, 4.8, 2.9 Hz, 3H), 1.3 (s, 3H), 1.1 (s, 3H).

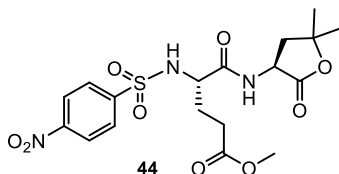


(S,S)-Methyl (4-hydroxy-4-methyl-2-((4-nitrophenyl)sulfonamido)pentanoyl)alaninate (42). Parent dipeptide Ns-Leu-Ala-OMe was oxidized to the title compound using **General Procedure C** (slow addition protocol) with an elevated oxidant modification using H₂O₂ (9.0 equiv) and Acetic Acid (1.0 equiv). The reaction was concentrated and purified via flash column chromatography on silica gel to afford the title compound as a white solid in 25% yield (37% recovered starting material). ¹H NMR (500 MHz, Chloroform-d) δ 8.3 (d, J = 8.6 Hz, 2H), 8.0 (d, J = 8.7 Hz, 2H), 6.6 (d, J = 7.9 Hz, 1H), 5.9 (d, J = 9.1 Hz, 1H), 4.4 – 4.2 (m, 1H), 3.7 (s, 3H), 3.7 – 3.6 (m, 1H), 3.1 (s, 1H), 1.4 (s, 3H), 1.2 (d, J = 7.2 Hz, 3H), 1.1 (s, 3H).

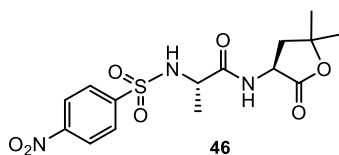


(S,S)-Methyl 5-((3-hydroxy-1-methoxy-3-methyl-1-oxobutan-2-yl)amino)-4-((4-nitrophenyl)sulfonamido)-5-oxopentanoate (43). Parent dipeptide Ns-Glu(OMe)-Val-OMe was oxidized to the title compound using **General Procedure C** (slow addition protocol) with an elevated oxidant modification using H₂O₂ (9.0 equiv) and Acetic Acid (1.0 equiv). The reaction was concentrated and purified via flash column chromatography on silica gel to afford the title compound as a white solid in

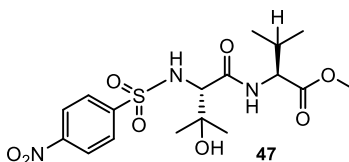
18% yield (49% recovered starting material). ^1H NMR (500 MHz, Chloroform- d) δ 8.3 (d, J = 8.8 Hz, 2H), 8.1 (d, J = 8.9 Hz, 2H), 7.2 (s, 1H), 6.5 – 6.4 (m, 1H), 4.3 (d, J = 8.8 Hz, 1H), 4.1 – 4.0 (m, 1H), 3.7 (s, 3H), 3.7 (s, 3H), 2.9 (s, 1H), 2.6 – 2.3 (m, 2H), 2.3 – 2.1 (m, 1H), 2.1 – 2.0 (m, 1H), 1.9 (td, J = 7.8, 7.0, 2.6 Hz, 1H), 1.2 (s, 3H), 1.0 (s, 3H).



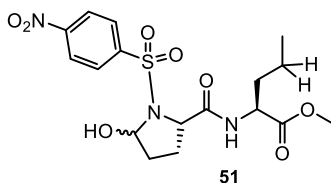
(S,S)-Methyl 5-((5,5-dimethyl-2-oxotetrahydrofuran-3-yl)amino)-4-((4-nitrophenyl)sulfonamido)-5-oxopentanoate (44). Parent dipeptide Ns-Glu(OMe)-Leu-OMe was oxidized to the title compound using **General Procedure C** (slow addition protocol) with an elevated oxidant modification using H_2O_2 (9.0 equiv) and Acetic Acid (1.0 equiv). The reaction was concentrated and purified via flash column chromatography on silica gel to afford the title compound as a white solid in 24% yield (40% recovered starting material). ^1H NMR (500 MHz, Acetone- d_6) δ 8.4 (d, J = 8.8 Hz, 2H), 8.1 (d, J = 8.9 Hz, 2H), 7.8 (d, J = 7.6 Hz, 1H), 7.2 (d, J = 8.9 Hz, 1H), 4.8 – 4.6 (m, 1H), 4.1 (td, J = 8.7, 5.5 Hz, 1H), 3.6 (s, 3H), 2.5 – 2.4 (m, 2H), 2.3 (dd, J = 12.4, 9.2 Hz, 1H), 2.0 – 2.0 (m, 1H), 2.0 – 1.8 (m, 2H), 1.4 (s, 3H), 1.4 (s, 3H).



(S,S)-N-(5,5-dimethyl-2-oxotetrahydrofuran-3-yl)-2-((4-nitrophenyl)sulfonamido)propanamide (46). Parent dipeptide Ns-Ala-Leu-OMe was oxidized to the title compound using **General Procedure C** (slow addition protocol) with an elevated oxidant modification using H_2O_2 (9.0 equiv) and Acetic Acid (1.0 equiv). The reaction was concentrated and purified via flash column chromatography on silica gel to afford the title compound as a white solid in 20% yield (37% recovered starting material). ^1H NMR (500 MHz, Acetone- d_6) δ 8.4 (d, J = 8.8 Hz, 2H), 8.1 (d, J = 8.9 Hz, 2H), 7.7 (d, J = 7.8 Hz, 1H), 7.2 (d, J = 8.5 Hz, 1H), 4.7 (ddd, J = 11.4, 9.2, 7.7 Hz, 1H), 4.2 – 3.9 (m, 1H), 3.8 (s, 1H), 2.4 (dd, J = 12.3, 9.2 Hz, 1H), 2.0 – 1.9 (m, 1H), 1.4 (s, 3H), 1.4 (s, 3H), 1.3 (d, J = 7.1 Hz, 3H).



(S,S)-Methyl (3-hydroxy-3-methyl-2-((4-nitrophenyl)sulfonamido)butanoyl)valinate (47). Parent dipeptide Ns-Val-Val-OMe was oxidized to the title compound using **General Procedure C** (slow addition protocol) with standard oxidant equivalents. The reaction was concentrated and purified via flash column chromatography on silica gel to afford the title compound as a white solid in 37% yield (51% recovered starting material). (12% by mass of a combination of other oxidized products were also isolated, but were inseparable by flash chromatography). ^1H NMR (500 MHz, Chloroform-*d*) δ 8.3 (d, *J* = 8.7 Hz, 2H), 8.1 (d, *J* = 8.7 Hz, 2H), 6.9 (d, *J* = 8.8 Hz, 1H), 6.4 (d, *J* = 9.3 Hz, 1H), 4.2 (dd, *J* = 8.9, 4.7 Hz, 1H), 3.8 (d, *J* = 9.4 Hz, 1H), 3.7 (s, 3H), 2.0 (dt, *J* = 7.1, 4.9 Hz, 1H), 1.4 (s, 3H), 1.1 (s, 3H), 0.7 (dd, *J* = 30.2, 6.8 Hz, 6H). ^{13}C NMR (126 MHz, Chloroform-*d*) δ 172.7, 169.4, 150.1, 145.5, 128.8, 124.3, 72.8, 63.7, 57.7, 52.7, 30.3, 27.7, 24.7, 18.9, 17.4 .



(S,S)-Methyl 2-(5-hydroxy-1-((4-nitrophenyl)sulfonyl)pyrrolidine-2-carboxamido)pentanoate (51). Parent dipeptide Ns-Pro-Nle-OMe was oxidized to the title compound using **General Procedure A** (iterative addition protocol). The reaction was concentrated and purified via flash column chromatography on silica gel to afford the title compound as a white solid in 37% yield (32% recovered starting material). The product was isolated as an inseparable mixture of diastereomers in a 5.4:1 ratio (major diast. peaks listed). ^1H NMR (500 MHz, Chloroform-*d*) δ 8.3 (d, *J* = 8.6 Hz, 2H), 8.1 (d, *J* = 8.4 Hz, 2H), 7.0 (d, *J* = 7.9 Hz, 1H), 5.8 – 5.7 (m, 1H), 4.6 – 4.4 (m, 1H), 4.3 (dd, *J* = 8.1, 4.2 Hz, 1H), 4.1 (d, *J* = 6.6 Hz, 1H), 3.7 (s, 3H), 2.3 – 2.1 (m, 2H), 1.9 (ddd, *J* = 11.7, 7.6, 4.1 Hz, 1H), 1.8 – 1.7 (m, 1H), 1.7 – 1.6 (m, 1H), 1.3 (ddd, *J* = 8.7, 6.1, 2.4 Hz, 2H), 0.9 (t, *J* = 7.3 Hz, 3H).

2.5 REFERENCES

¹ Chem and Eng News: Business. **2005**, *83*, 17-24.

² (a) Rella, M. R. and Williard, P. G. *J. Org. Chem.*, **2007**, *72*, 525-531. (b) Saladin, R.; Mezzetti, M.; Mincione, R.; Torrini, I.; Paradisi, M. P.; and Mastropietro, G. *J. Org. Chem.* **1999**, *64*, 8468-8474. (c) Annese, C.; D'Accolti, L.; De Zotti, M.; Fusco, C.; Toniolo, C.; Williard, P. G.; and Curci, R. *J. Org. Chem.* **2010**, *75*, 4812-4816.

³ Dangel, B. D.; Johnson, J. A.; and Sames, D. *J. Am. Chem. Soc.* **2001**, *123*, 8149-8150.

⁴ (a) Young, T. S. and Schultz, P. G. *J. Biological Chem.* **2010**, *285*, 11039-44. (b) Liu, C. C. and Schultz, P. G. *Annu. Rev. Biochem.* **2010**, *79*, 413-44.